© 2018. Published by The Company of Biologists Ltd | Development (2018) 145, dev164285. doi:10.1242/dev.164285

STEM CELLS AND REGENERATION

RESEARCH ARTICLE

Pvr receptor tyrosine kinase signaling promotes post-embryonic morphogenesis, and survival of glia and neural progenitor cells in *Drosophila*

Renee D. Read*

ABSTRACT

Stem cells reside in specialized microenvironments, called niches, that regulate their development and the development of their progeny. However, the development and maintenance of niches are poorly understood. In the *Drosophila* brain, cortex glial cells provide a niche that promotes self-renewal and proliferation of neural stem cell-like cells (neuroblasts). In the central brain, neuroblasts and their progeny control post-embryonic morphogenesis of cortex glia through PDGF-like ligands, and this PDGFR receptor tyrosine kinase (RTK) signaling in cortex glia is required for expression of DE-cadherin, which sustains neuroblasts. Thus, through an RTK-dependent feed-forward loop, neuroblasts and their glial niche actively maintain each other. When the EGFR RTK is constitutively activated in cortex glia, they overexpress PDGF orthologs to stimulate autocrine PDGFR signaling, which uncouples their growth and survival from neuroblasts, and drives neoplastic glial transformation and elimination of neuroblasts. These results provide fundamental insights into glial development and niche regulation, and show that niche-neural stem cell feed-forward signaling becomes hijacked to drive neural tumorigenesis.

KEY WORDS: Niche, Glia, Neuroblast, PDGFR, *Drosophila melanogaster*, Gliomagenesis

INTRODUCTION

In the mammalian central nervous system (CNS), neuro-glial stem/progenitor cells give rise to neurons and glia, and are maintained in distinct microenvironments called niches (reviewed by Bjornsson et al., 2015). In the niche, neuro-glial stem/progenitor cells are regulated by local and systemic cues that promote their self-renewal and modulate their proliferation and differentiation. Niche microenvironments are found in the subventricular zone and other neurogenic regions, and they are composed of multiple cell types (Bjornsson et al., 2015). This complexity endows niches with an ability to respond to local and systemic cues, but makes the interactions between niche cells and neuro-glial stem cells complicated to study. A deeper understanding of the contribution of various cell types to niche function and development may bring novel insights into the cellular origins of neurological diseases.

The *Drosophila* CNS, which has a simpler cellular composition than the mammalian CNS, is a powerful model for investigating interactions between neural-glial stem/progenitor cells and the neurogenic niche. The *Drosophila* brain and nerve cord are analogous to the mammalian brain and spinal cord, and are derived from stem-like neuro-glial progenitor cells called neuroblasts, which arise from embryonic neuroepithelia and divide asymmetrically to generate neurons and glia (reviewed by Doe, 2008; Homem and Knoblich, 2012). The *Drosophila* central brain is generated by neuroblasts that enter a first period of neurogenesis during embryonic development and a second period of post-embryonic neurogenesis during larval development (Fig. 1A), separated by a period of cell-cycle arrest. Post-embryonic neurogenesis is regulated by two classes of glia that contribute to the niche (Chell and Brand, 2010; Dumstrei et al., 2003; Sousa-Nunes et al., 2011; Spéder and Brand, 2014). One class of niche glia, subperineurial glia, creates the blood-brain barrier and responds to systemic nutritional cues (Spéder and Brand, 2014). Another class of niche glia, cortex glia, is large and extends processes to contact overlying subperineurial glia and wrap the cell bodies of individual neuroblasts and their daughter neurons (Fig. 1B). Cortex glia thereby create local microenvironments that are required for neuroblast maintenance and neuronal maturation (Coutinho-Budd et al., 2017; Dumstrei et al., 2003; Pereanu et al., 2005; Spéder and Brand, 2018).

In *Drosophila*, post-embryonic neurogenesis begins when neuroblasts exit from quiescence during early larval development, beginning in late 1st and early 2nd instar stages, to re-enter the cell cycle (Fig. 1A). Neuroblast cell cycle re-entry is triggered by expression of secreted insulin-like peptides (Dilps), such as Dilp6, by subperineurial glia in response to nutrient-dependent systemic signals (Chell and Brand, 2010; Spéder and Brand, 2018). Dilps activate insulin-like receptor (InR) in neuroblasts, leading to phosphatidylinositol 3-kinase (PI3K) signaling and cell cycle re-entry (Chell and Brand, 2010; Sousa-Nunes et al., 2011), and activate InR in cortex glia to initiate neuroblast wrapping (Spéder and Brand, 2018). During later larval development, cortex glia continue to express Dilp6, which is thought to sustain InR-driven neuroblast and glial proliferation (Avet-Rochex et al., 2012; Sousa-Nunes et al., 2011). In later larval stages, continued PI3K-dependent neuroblast proliferation is stimulated by cortex glia through secretion of Jellybelly (Jeb), which is a ligand for the Alk receptor tyrosine kinase (RTK) expressed by neuroblasts (Cheng et al., 2011). Yet how interactions between neuroblasts and glia regulate formation and function of the glial niche remains poorly understood.

To discover new pathways required cell-autonomously in glia for post-embryonic neurogenesis, I performed a *Drosophila* glia-specific RNAi screen. This approach identified a mechanism whereby the PDGFR ortholog Pvr and its ligands mediate paracrine signaling between cortex glia and central brain neuroblasts and their progeny to promote and sustain post-embryonic neurogenesis. I also found that,

Department of Pharmacology, Emory University School of Medicine, Atlanta, GA 30322, USA.

*Author for correspondence (renee.read@emory.edu)

R.D.R., 0000-0002-5594-6958

Received 8 February 2018; Accepted 10 October 2018

Development (2018) 145, dev164285. doi:10.1242/dev.164285

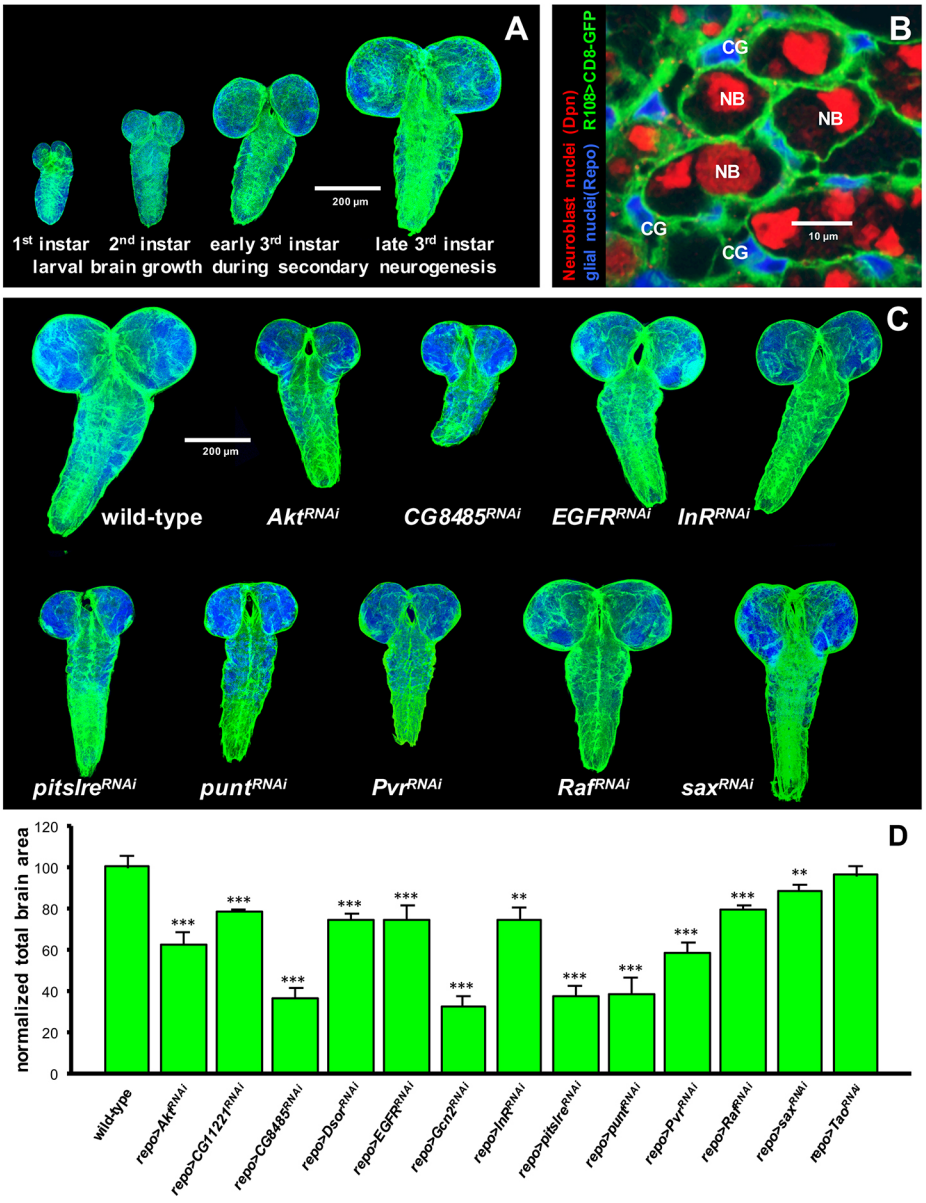

Fig. 1. Glial-specific non-autonomous regulation of post-embryonic brain growth. (A) Optical projections of whole wild-type brain-nerve cord complexes (same scale). Dorsal view; anterior upwards. *repo>CD8-GFP* labels glial cell membranes; blue labels cell nuclei. (B) Optical sections (2 µm) of the cortex glia niche in the central brain in a 3rd instar larva. Cortex glial cell membranes labeled by CD8-GFP expression driven by *R108-Gal4*; the glial-specific Repo transcription factor (blue) labels cortex glia (CG) nuclei; the neuroblast-specific Dpn transcription factor (red) labels neuroblast nuclei (NB). (C) Late 3rd instar brains at ∼130 h AED (same scale). Blue labels cell nuclei. *repo>CD8-GFP* labels all glia. (D) Brain area measured in µm^2 in optical projections of late 3rd instar brains, normalized to wild type; three or four brains measured for each genotype. Glial-specific expression of all indicated RNAi constructs, driven by *repo-Gal4*, noticeably reduced brain size when compared with wild-type controls (see Table S1). Values for each RNAi construct compared with wild type using Student's two-tailed *t*-tests; $^{**}P<0.05$, $^{***}P<0.005$.

in the context of gain-of-function RTKs, Pvr signaling becomes hijacked to drive tumorigenic transformation of cortex glia, in a process similar to tumorigenic transformation of human glia. These results establish that PDGFR signaling plays evolutionarily conserved roles in glial development and tumorigenesis.

RESULTS

A screen for genes required for glial-specific regulation of post-embryonic brain growth

To identify new genes required in glia for post-embryonic neurogenesis, I performed an RNAi screen. I screened 553 Gal4-UAS-dependent RNAi constructs targeting 223 of the 243 kinases in the fly genome in order to enrich for signaling pathways (Read et al., 2013). RNAi constructs were expressed specifically in glia during development using the pan-glial *repo-Gal4* transcriptional driver and tested for phenotypic effects on larval brain growth. Brain growth phenotypes were confirmed by confocal microscopy (Fig. 1C,D). RNAi constructs that yielded small brains in late stage larvae were subsequently screened for cell-type specificity: these RNAi constructs were overexpressed in neuroblasts and other proliferative neural cells to distinguish RNAi constructs that caused glial-specific growth phenotypes (Table S1; Fig. S1). From this screen, I identified 14 candidate genes for which restricted RNAi in glia preferentially reduced larval brain growth (Fig. 1E; Table S1). Candidate genes were classified using FlyBase, Gene Ontology and KEGG pathways (Table S1), which showed that kinases with core functions in PI3K signaling and/or in nutritional metabolism were most highly represented, consistent with known requirements for PI3K signaling and nutrient availability in neuroblast re-activation and post-embryonic neurogenesis (Chell and Brand, 2010; Sousa-Nunes et al., 2011; Spéder and Brand, 2018). For select candidate genes, the phenotypic effects of glial-specific kinase loss of function was confirmed by testing multiple RNAi constructs, dominant-negative constructs and/or mutant alleles, if available (Table S1). I found that glial-specific loss of Pvr, which encodes the sole *Drosophila* ortholog of the vertebrate VEGFR and PDGFR RTKs (Cho et al., 2002; Duchek et al., 2001; Heino et al., 2001), strongly reduced brain growth.

Development (2018) 145, dev164285. doi:10.1242/dev.164285

Pvr activity is required in cortex glia for neuroblast proliferation and neuron survival

Glial-specific Pvr knockdown (*repo>Pvr^{RNAi}*) impaired larval brain growth. *Pvr* mRNA expression was not detectable by qPCR on *repo>Pvr^{RNAi}* 3rd instar brains (not shown), demonstrating that *Pvr* mRNA was knocked down. Brain growth defects in *repo>Pvr^{RNAi}* animals were enhanced by Dicer co-overexpression (improves RNAi) and by a Pvr heterozygous mutant background, showing that Pvr gene function can be further reduced to further hamper brain growth (Fig. 2A). I did not observe obvious molting delays in *repo>Pvr^{RNAi}* animals (Fig. S2), indicating that defects were not due to organism-wide developmental delays. Brain size phenotypes caused by Pvr loss were glial specific: overexpression of Pvr RNAi constructs in neuroblasts or neurons caused no discernible gross defects (Table S1; Fig. S1B-E). This is consistent with observations that neuroblast clones homozygous for loss-of-function Pvr alleles showed no gross defects (not shown). Notably, glial-specific overexpression of dominant negative Pvr (Pvr$^{\Delta C}$, Brückner et al., 2004) in a *Pvr* heterozygous null mutant background reduced brain growth and reduced neuroblasts, neurons and glial cells compared with wild type (Fig. 2A,H,J; Fig. S3A,B).

To determine how glial-specific Pvr loss-of-function causes brain defects, I examined development of *repo>Pvr^{RNAi}* brains. About 8-10 h after hatching, in late 1st to early 2nd instar stages, neuroblasts normally undergo reactivation and re-enter the cell cycle to begin post-embryonic neurogenesis (Britton and Edgar, 1998; Chell and Brand, 2010; Sousa-Nunes et al., 2011). Brains of 1st instar animals showed no differences in size or glial morphology or glial cell numbers compared with wild-type controls (Fig. S4A-D,K), suggesting that embryonic brain development proceeds normally in *repo>Pvr^{RNAi}* animals, perhaps because of a lack of RNAi efficacy at early stages. Early 2nd instar *repo>Pvr^{RNAi}* brains appeared grossly normal, but showed defects in cortex glia cell morphologies, reduced cortex glia cell numbers and a slight, but not statistically significant, decrease in overall proliferation (Fig. 2B,C; Fig. S4A,B,E,F,L). By the late 3rd instar, during normal development, the brain dramatically enlarges by accumulation of new neurons born from neuroblasts and ganglion mother cells (GMCs), which are intermediate neuronal progenitor cells derived from neuroblasts (Fig. 1A). By the 3rd instar, glial-specific Pvr-RNAi or dominant-negative Pvr significantly reduced numbers of several cell types due to defects in cell proliferation and survival (Fig. 2B-L). Glial-specific Pvr-RNAi or dominant-negative Pvr significantly reduced proliferation in the central brain compared with controls, as revealed by EdU incorporation and phospho-histone-H3 staining cells, with *repo>Pvr$^{\Delta C}$* brains showing reduced numbers of mitotic neuroblasts compared with wild type (Fig. 2C-D). Apoptotic neuroblasts were also present in the central brain (Fig. 2I-L; Fig. S5), and comprised 3% and 2% of the TUNEL-positive cells detected in *repo>Pvr^{RNAi}* and *repo>Pvr$^{\Delta C}$* animals, respectively. TUNEL-positive immature neurons were more common (Fig. 2I-L; Fig. S5) and comprised 65% and 54% of the TUNEL-positive cells detected in *repo>Pvr^{RNAi}* and *repo>Pvr$^{\Delta C}$* animals, respectively. Of note, differential loss of type I or type II neuroblasts was not observed, determined by staining for markers such as Ase (not shown). Thus, glial-specific Pvr loss of function depressed brain growth through reduced proliferation and apoptosis of neuroblasts and immature neurons.

Pvr knockdown induced prominent cortex glia cell loss and morphogenesis defects by the 3rd instar, resulting in reduced cortex glia membrane processes wrapping neuroblasts and immature neurons in the central brain (Fig. 2E-I; Fig. S4B-M). Similar phenotypes were observed in *repo>Pvr$^{\Delta C}$; Pvr$^{c02195/+}$* mutants (Fig. S2A,B). Previous studies indicated that cortex glia in the larval central brain undergo limited proliferation (Avet-Rochex et al., 2012), which was only slightly reduced by Pvr RNAi (Fig. S6). However, blocking cell cycle in glia does not induce glial morphogenesis defects or reduce brain size comparable with the *repo>Pvr^{RNAi}* phenotype (Read et al., 2009; Spéder and Brand, 2018). Instead, cortex glia were reduced by apoptosis: pyknotic cortex glia and TUNEL-positive cortex glia were evident in the central brain of *repo>Pvr^{RNAi}* and *repo>Pvr$^{\Delta C}$* animals (31% and 45% of all TUNEL-positive cells detected, respectively) (Fig. 2J-L; Fig. S4I,J; Fig. S5). *Pvr* loss also caused reduced expression of cell-type specific transcription factors, such as SoxN and PntP2, which are expressed in wild-type cortex glia (Fig. S7A-F) (Avet-Rochex et al., 2012). SoxN is the closest *Drosophila* ortholog of the mammalian SOX2 transcription factor, a marker for neuro-glial stem/progenitor cells (McKimmie et al., 2005), which, based on RNAi phenotypes, is required for development of cortex glia (not shown). Thus, Pvr function is required for survival and morphogenesis of cortex glia in the central brain.

To independently determine whether Pvr signaling is required for brain development, I examined phenotypes of loss-of-function mutants of *Pvf1*, *Pvf2* and *Pvf3*, which encode Pvr ligands. The Pvfs are semi-redundant, and *Pvf* single mutants are viable and show no obvious brain phenotypes (not shown). Double *Pvf2$^{-/-}$;Pvf3$^{-/-}$* (*Pvf2-3$^{-/-}$* dual deletion) and *Pvf1^{ex3};Pvf2-3$^{-/-}$* triple mutants are early lethal, but this lethality is rescued by expressing Pvf2 or constitutively active Pvr (*Pvr$^{\lambda}$*, Pvr fused to a lambda dimerization domain) specifically in hemacytes using *crq-Gal4* (Parsons and Foley, 2013). *Pvf2-3$^{-/-}$crq>Pvf2* double mutants survive to adulthood, and show slight brain morphogenesis defects (not shown). *Pvf1^{ex3};Pvf2-3$^{-/-}$crq>Pvr$^{\lambda}$* and *Pvf1^{ex3};Pvf2-3$^{-/-}$crq>Pvf2* triple mutants survive to pupal stages, and showed neuroblast loss and reduced neurogenesis in the central brain relative to wild type during larval development (Fig. 2A,C,H; Fig. S3C,D). UAS-GFP reporters were included in these genotypes to confirm that *crq-Gal4* was expressed in hemacytes and not in glia or neurons; some larvae showed *crq-Gal4*-driven GFP expression in scattered ensheathing glia and hemacytes in the CNS, but showed brain phenotypes (Fig. 2A). To label cortex glia in triple *Pvf* mutants, I used a Pax6-EGFP reporter (Metaxakis et al., 2005), which is expressed in cortex glia (Fig. S3C,D; Fig. S8A). Both *Pvf1^{ex3};Pvf2-3$^{-/-}$crq>Pvr$^{\lambda}$* and *Pvf1^{ex3};Pvf2-3$^{-/-}$crq>Pvf2* triple mutant 3rd instar larvae showed reduced cortex glial cell numbers, reduced cortex glial processes in the central brain and defects in brain morphogenesis (Fig. 2A; Fig. S3C,D). In contrast, larval brain phenotypes were not examined in *Pvr* mutants because no viable larvae were obtained from the five loss-of-function alleles tested, even when *Pvr* was rescued by *crq-Gal4* (Parsons and Foley, 2013), and no central brain-specific *Pvr* homozygous mutant glial clones or Pvr-RNAi glial clones were recovered (not shown).

Pvr protein is strongly expressed in cortex glia in the central brain in early and late stage larvae (Fig. 3A-D). *Pvr* gene traps, with GFP or Gal4-containing transposons inserted into the *Pvr* locus, are also expressed in cortex glia (Fig. S9). To test whether Pvr functions specifically in cortex glia, I used cortex glia-specific Gal4 drivers (*R108-Gal4* or *R122-Gal4,* Fig. S8B,C) to overexpress Pvr^{RNAi}, which reduced neuroblast and cortex glial cell numbers, and decreased larval brain size, which is indicative of fewer neurons (Fig. 3E-H). In *R122>Pvr^{RNAi}* central larval brains, cortex glial processes were reduced (Fig. 3E-I). *R122>Pvr$^{\Delta C}$* animals also showed similar defects, including neuroblast loss and defective cortex glia morphogenesis (Fig. S10A-C). Overexpression of Pvr RNAi

Development (2018) 145, dev164285. doi:10.1242/dev.164285

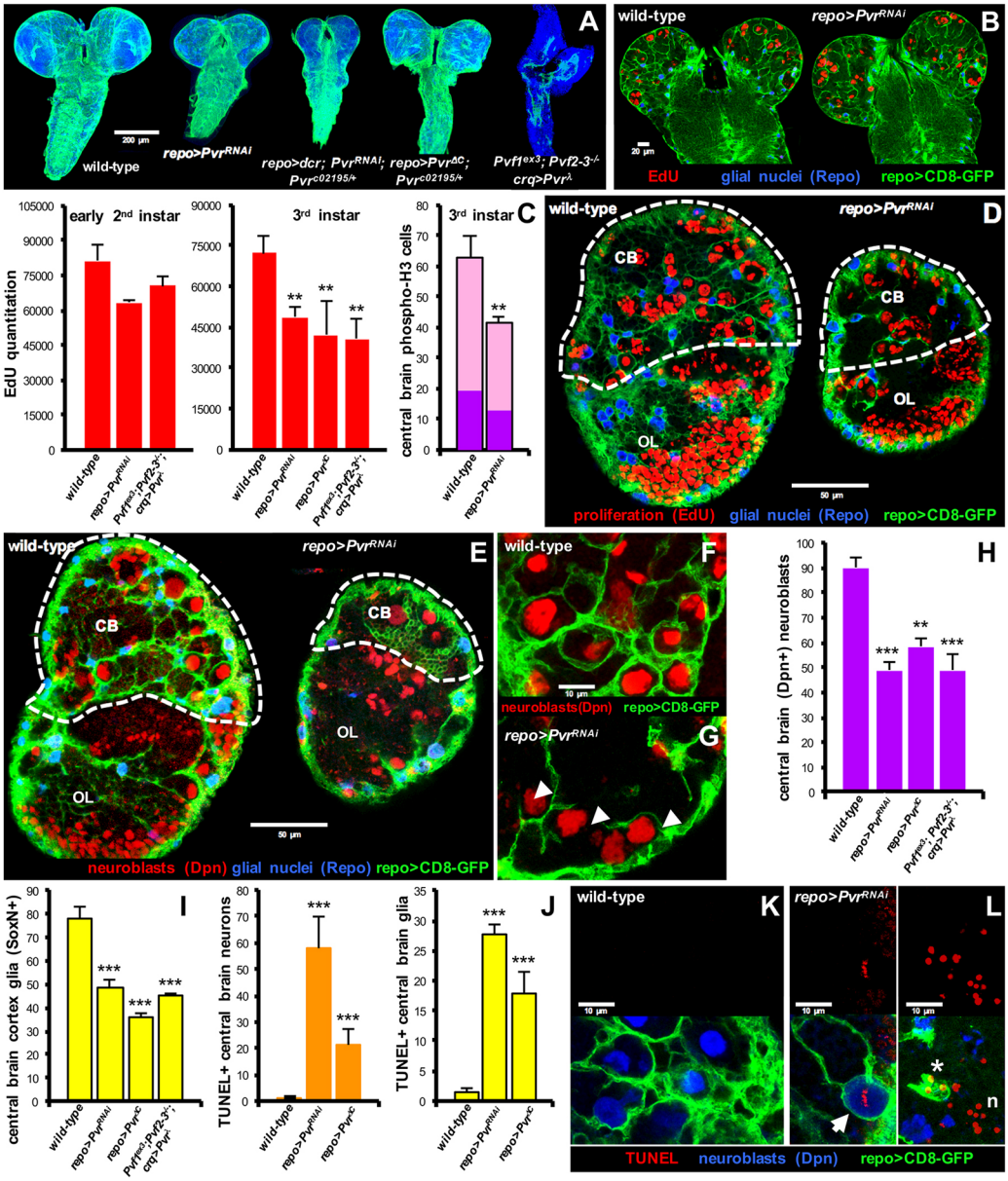

Fig. 2. Pvr and Pvfs are required for larval neuroblast proliferation and maintenance. (A) Late 3rd instar brains at ∼130 h AED (same scale). Blue labels cell nuclei. *repo>CD8-GFP* labels glial cell membranes in wild-type, *repo>Pvr^{RNAi}*, *repo>dcr;Pvr^{RNAi};Pvr$^{c02195/+}$* and *repo>Pvr$^{\Delta C}$;Pvr$^{c02195/+}$* brains. In *Pvf1^{ex3};Pvf2-3$^{-/-}$crq>Pvr$^{\lambda}$* brains, CD8-GFP expressed by *crq-Gal4* labels hemacytes and scattered ensheathing glia. (B) Early 2nd instar brains, at onset of post-embryonic neurogenesis. EdU (red) labels S-phase and M-phase cells. *repo>CD8-GFP* labels glia; Repo (blue) labels glial nuclei. (C) Total pixels for EdU labeling in whole early 2nd instar brains computed from confocal *z*-stacks: wild type (n=5), *repo>Pvr^{RNAi}* (n=4), *Pvf1^{ex3};Pvf2-3$^{-/-}$crq>Pvr$^{\lambda}$* (n=3). Total pixels for EdU-labeling in the central brain of late 3rd instar brain hemispheres computed from 25 µm confocal *z*-stacks: wild type (n=3), *repo>Pvr^{RNAi}* (n=5), *repo>Pvr$^{\Delta C}$;Pvr$^{C02195/+}$* (n=3), *Pvf1^{ex3};Pvf2-3$^{-/-}$crq>Pvr$^{\lambda}$* (n=3). Total phospho-Histone-H3-positive cells in the central brain counted in 30 µm confocal *z*-stacks of late 3rd instar brain hemispheres, with dark purple indicating phospho-Histone-H3-positive Dpn^{+} neuroblasts: wild type (n=5), *repo>Pvr^{RNAi}* (n=4). Values for each genotype compared with wild-type controls with Student's two-tailed *t*-test, which showed no statistically significant difference in early 2nd instars, but showed statistically significant differences in 3rd instars. (D,E) Optical sections (2 µm) of 3rd instar brain hemispheres. *repo>CD8-GFP* labels glia; Repo (blue) labels glial cell nuclei; red labels EdU^{+} cells (D) or Dpn-positive neuroblasts (E). Dashed lines outline the central brain (CB) relative to the optic lobe (OL). *repo>Pvr^{RNAi}* brains showed decreased size, reduced glial processes and reduced EdU^{+} cells and Dpn^{+} cells compared with wild-type controls. (F,G) Higher-magnification views of the cortex glial niche in wild-type brains (F), in which neuroblasts (red Dpn^{+} nuclei) are normally fully wrapped by cortex glial cell membranes (green); in *repo>Pvr^{RNAi}* brains (G), however, cortex glial cell membranes fail to fully wrap neuroblasts (arrows). (H,I) Neuroblasts (Dpn^{+}) in the central brain counted in 20 µm confocal *z*-stacks of late 3rd instar brain hemispheres: wild type (n=8), *repo>Pvr^{RNAi}* (n=4), *repo>Pvr$^{\Delta C}$;Pvr$^{C02195/+}$* (n=4), *Pvf1^{ex3};Pvf2-3$^{-/-}$crq>Pvr$^{\lambda}$* (n=4). Cortex glia (SoxN^{+}) in the central brain counted in 20 µm confocal *z*-stacks of late 3rd instar brain hemispheres: wild type (n=9), *repo>Pvr^{RNAi}* (n=4), *repo>Pvr$^{\Delta C}$;Pvr$^{c02195/+}$* (n=4), *Pvf1^{ex3};Pvf2-3$^{-/-}$crq>Pvr$^{\lambda}$* (n=3). Values for each mutant compared with wild type using Student's two-tailed *t*-test, which showed that loss of Pvr signaling is significantly associated with loss of neuroblasts and cortex glia. (J) TUNEL-positive neurons and cortex glia in the central brain counted in 30 µm confocal *z*-stacks of 3rd instar brain hemispheres: wild type (n=5), *repo>Pvr^{RNAi}* (n=5), *repo>Pvr$^{\Delta C}$;Pvr$^{c02195/+}$* (n=4). Values for each mutant compared with wild type using Student's two-tailed *t*-test, which showed that loss of Pvr signaling is significantly associated with apoptosis of neurons and cortex glia. (K,L) Optical sections (3 µm) of the central brain in 3rd instar larvae. *repo>CD8-GFP* labels glia; Dpn (blue) labels neuroblast nuclei; red labels TUNEL^{+} cells in wild-type (K, left) and *repo>Pvr^{RNAi}* (K, right) brains. TUNEL^{+} neuroblasts (arrow), cortex glia (asterisk) and neurons (n) were present in *repo>Pvr^{RNAi}* (L) brains, but not wild type. Full hemispheres are shown in Fig. S5. **P<0.05; ***P<0.005. Data are mean±s.e.m.

Development (2018) 145, dev164285. doi:10.1242/dev.164285

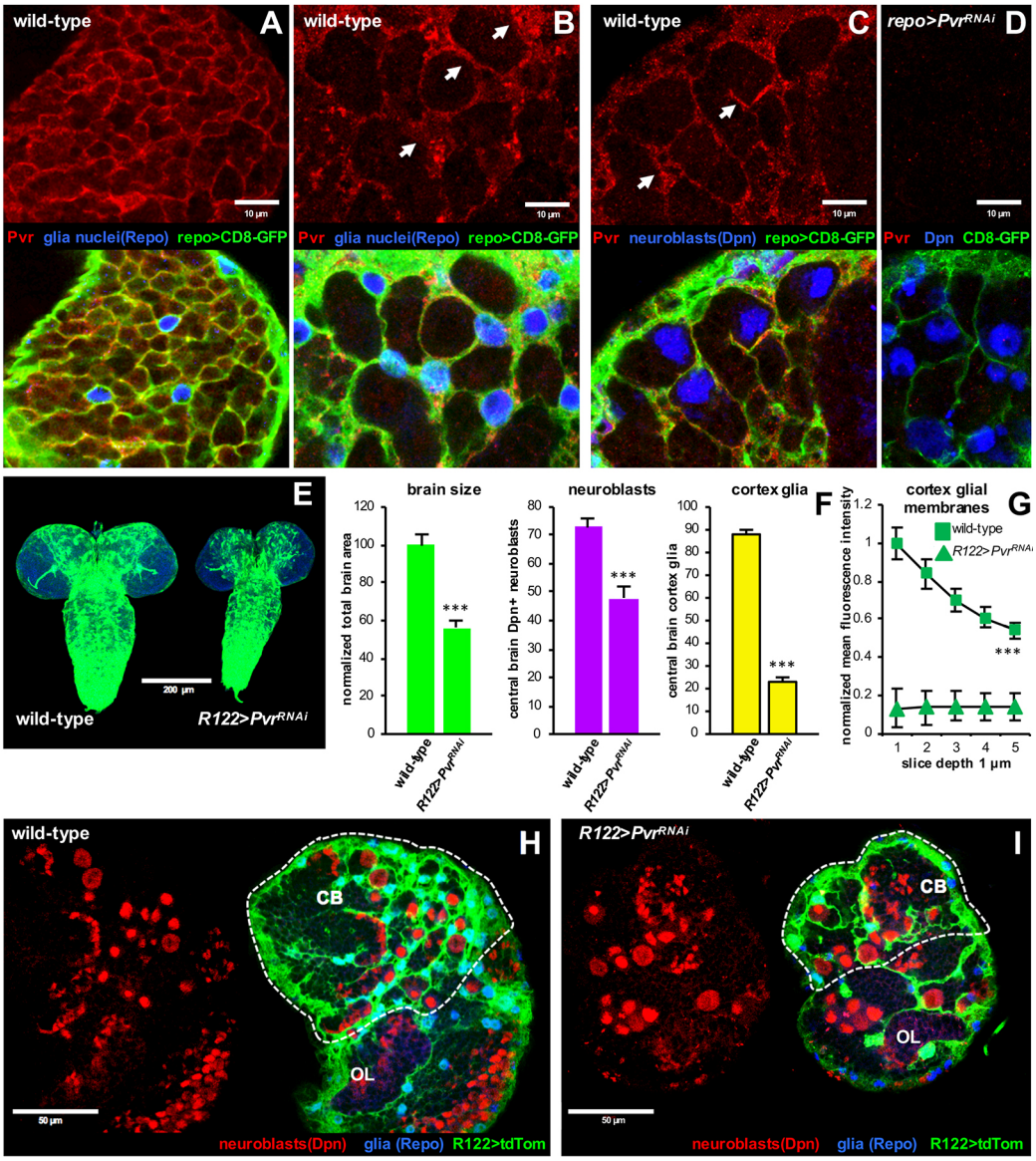

Fig. 3. Pvr activity is required in cortex glia. (A-D) Optical sections (2 µm) of the central brain of (A) late 1st instar and (B,C) early 3rd instar wild-type larvae or (D) 3rd instar *repo>Pvr*^{RNAi} larvae. (A,B) Repo (blue) labels glial nuclei. (C,D) Dpn (blue) labels neuroblast nuclei. (A-C) Pvr protein (red) expression overlaps with cortex glial cell membranes and processes (labeled by *repo>CD8-GFP*) that wrap neuroblasts and immature neurons (arrows). (D) Pvr staining (red) is lost upon Pvr knockdown. (E) Late 3rd instar brains at ∼130 h AED (same scale). Blue labels cell nuclei. Cortex glia labeled with membrane-associated-RFP (tdTom) driven by *R122-Gal4* (false-colored green). (F) Brain area measured in µm^2 in optical projections of late 3rd instar brains, normalized to wild type: wild type (*n*=4), *R122>Pvr*^{RNAi} (*n*=3). Neuroblasts (Dpn$^+$ cells) in the central brain counted in 20 µm confocal *z*-stacks of late 3rd instar brain hemispheres: wild type (*n*=3), *R122>Pvr*^{RNAi} (*n*=3). Cortex glia (R122>tdTom Repo$^+$) in the central brain counted in 20 µm confocal *z*-stacks of late 3rd instar brain hemispheres: wild-type (*n*=3), *R122>Pvr*^{RNA} (*n*=3). ***P<0.005. (G) Cell membrane fluorescence intensities of cortex glia associated with neuroblasts in the central brain, normalized to wild type, plotted over a 5 µm depth: mean intensities are significantly different between wild type (*n*=4) and *R122>Pvr*^{RNAi} (*n*=4), determined using paired Student's *t*-test. ***P<0.005. (H,I) Optical sections (2 µm) of age-matched 3rd instar brains. *R122>tdTom* (green) labels cortex glia; Repo (blue) labels glial cell nuclei; Dpn labels neuroblast nuclei (red). Dashed lines outline the central brain (CB) relative to the optic lobe (OL). *R122>Pvr*^{RNAi} brains showed decreased size, reduced glial processes and reduced Dpn$^+$ cells compared with wild type.

constructs in other glia subtypes, such as astrocyte-like glia (*alarm-Gal4*), perineurial glia (*NP6293-Gal4*) or subperineurial glia (*moody-Gal4, NP2276-Gal4*) (Awasaki et al., 2008; Bainton et al., 2005; Doherty et al., 2009), combined with Dcr, yielded viable animals that had grossly normal brain and glial phenotypes (Fig. S11), indicating that effects of Pvr loss were specific to cortex glia.

Pvf expression is required in neuroblasts and their progeny

To understand Pvr function in post-embryonic brain development, I determined which cells express Pvfs. Staining using a published validated Pvf1 antibody showed Pvf1 predominantly present in central brain neuroblasts and cortex glia (Rosin et al., 2004) (Fig. 4A). Pvf1 protein observed in cortex glia is likely receptor bound, as Pvf1 staining on cortex glia was reduced in *repo>Pvr*^{RNAi} animals (Fig. S12). Because no Pvf2 antibody was available, a *Pvf2-lacZ* promoter fusion reporter was used to determine expression patterns: *Pvf2-lacZ* is expressed in central brain neuroblasts and their neighboring daughter cells (Choi et al., 2008), likely GMCs (Fig. 4B-F). Pvf2-LacZ expression begins in late 1st instar/early 2nd instar co-incident with neuroblast cell cycle re-entry, as evidenced

Development (2018) 145, dev164285. doi:10.1242/dev.164285

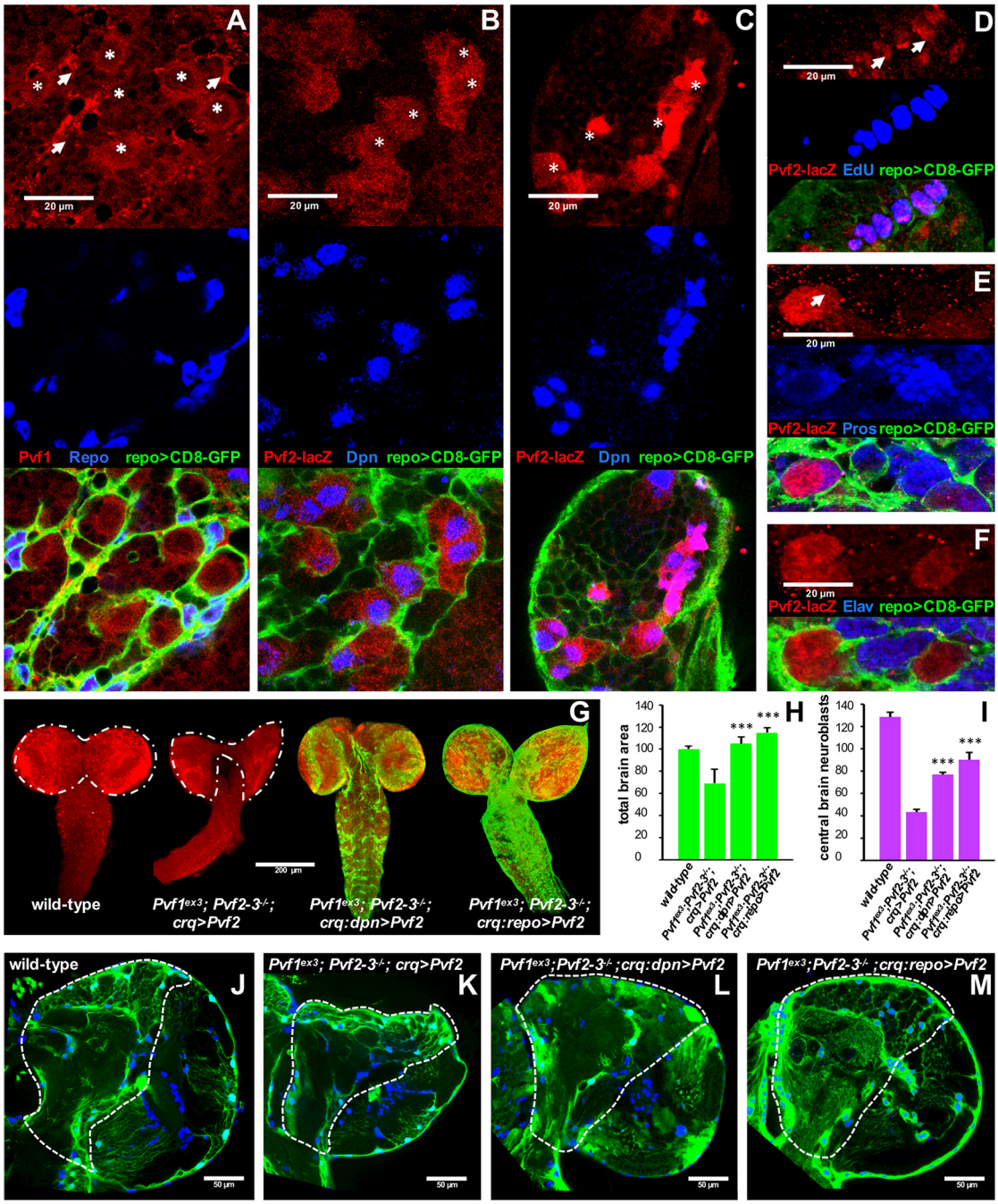

Fig. 4. Pvf expression is required in neuroblasts for their proliferation and maintenance. (A) Optical sections (2 µm) of a wild-type 3rd instar central brain. Pvf1 protein expression (red) outlines neuroblast cell bodies (asterisks). Pvf1 is also detected on cortex glial processes (arrows, overlay). *R122>CD8-GFP* labels cortex glia; Repo (blue) labels glial nuclei. (B,C) Optical projections (4 µm) of the central brain from *Pvf2-lacZ* wild-type 3rd instar (B) or early 2nd instar (C) brains. *LacZ* (red) is strongly expressed in neuroblasts (Dpn, blue, purple in overlays, asterisks show examples) and neighboring daughter cells. *repo>CD8-GFP* labels glia. (D) Optical projection (12 µm) of an early 2nd instar wild-type brain with *Pvf2-lacZ*. *LacZ* (red) is strongly expressed in EdU-labeled cells (blue, purple in overlay), which have re-entered the cell cycle (arrows). *repo>CD8-GFP* labels glia. (E,F) Optical projection (2 µm) of 3rd instar wild-type brains with *Pvf2-lacZ*. (E) *LacZ* (red) is strongly expressed in GMCs and immature neurons (labeled by Pros, blue, purple in overlay) adjacent to a neuroblast (arrow). (F) *LacZ* (red) is not expressed in differentiated neurons (labeled by Elav, blue). *repo>CD8-GFP* labels glia. (G) Whole 3rd instar larval brains at ∼130 h AED; same scale. Dpn (red) labels neuroblasts. Dashed lines outline the brain lobes of a wild-type brain (left) and a *Pvf1*^{ex3}*;Pvf2-3*$^{-/-}$*;crq>Pvf2* mutant (right). CD8-GFP visualizes brain size and expression patterns of *dpn-Gal4* and *repo-Gal4* drivers used to rescue *Pvf1*^{ex3}*;Pvf2-3*$^{-/-}$*;crq>Pvf2* mutants. (H) Brain area measured in µm^2 in optical projections of late 3rd instar brains, normalized to wild type: wild type (*n*=7), *Pvf1*^{ex3}*;Pvf2-3*$^{-/-}$*crq>Pvf2* (*n*=6), *Pvf1*^{ex3}*;Pvf2-3*$^{-/-}$*;crq>Pvf2;repo>Pvf2* (*n*=6), *Pvf1*^{ex3}*;Pvf2-3*$^{-/-}$*;crq>Pvf2;repo>Pvf2* (*n*=4). (I) Neuroblasts (Dpn$^+$) in the central brain counted in 50 µm confocal *z*-stacks of 3rd instar brain hemispheres: wild type (*n*=3), *Pvf1*^{ex3}*;Pvf2-3*$^{-/-}$*crq>Pvf2* (*n*=3), *Pvf1*^{ex3}*;Pvf2-3*$^{-/-}$*;crq>Pvf2;dpn>Pvf2* (*n*=4), *Pvf1*^{ex3}*;Pvf2-3*$^{-/-}$*;crq>Pvf2;repo>Pvf2* (*n*=3). *Pvf1*^{ex3}*;Pvf2-3*$^{-/-}$*;crq>Pvf2; repo>Pvf2* and *Pvf1*^{ex3}*;Pvf2-3*$^{-/-}$*;crq>Pvf2;repo>Pvf2* mutant brains showed significant increases in size and neuroblast number compared with *Pvf1*^{ex3}*;Pvf2-3*$^{-/-}$*;crq>Pvf2* controls. Samples compared pair-wise with Student's two-tailed *t*-tests; ***P<0.005. (J-M). Optical sections (3 µm) of mid-way through 3rd instar brains (same scale). *Pvf1*^{ex3}*;Pvf2-3*$^{-/-}$*crq>Pvf2* animals (K) showed a small central brain (dashed lines) relative to wild type (J), which was rescued by Pvf2 overexpressed by *dpn-Gal4* or *repo-Gal4* (L,M). Glia labeled with *Pax6-EGFP* (K); glia labeled with *repo>CD8-GFP* (J,M); neuroblasts and their progeny labeled with *dpn>CD8-GFP* (L); Repo (blue) labels glial nuclei.

Development (2018) 145, dev164285. doi:10.1242/dev.164285

by EdU incorporation, and continues into 2nd and 3rd instar stages (Fig. 4B-F). In contrast, low to no Pvf3 staining was detected using published Pvf3 antibodies (Rosin et al., 2004). In lieu of antibody staining, I examined expression patterns of several Gal4 reporters with *Pvf2* and *Pvf3* promoter fragments (R77E03, R77E04, R77E08), which showed strong expression in overlapping populations of central brain neuroblasts and weaker expression in daughter neurons (http://flweb.janelia.org/cgi-bin/flew.cgi) (Li et al., 2014). Data from these Gal4 reporters are consistent with presence of neuroblast-specific regulatory elements, although they do not contain full-length *Pvf2* and *Pvf3* promoters so we can only draw limited conclusions. These data indicate that *Pvf1* and *Pvf2* are expressed by neuroblasts and more weakly by neighboring GMCs.

These results suggest that Pvfs are required in neuroblasts and their progeny to promote development of cortex glia. Confirming this hypothesis, overexpressing *Pvf2* with *dpn-Gal4*, which drives transgene expression in neuroblasts and GMCs, partially rescued central brain neuroblasts and gross brain growth and morphology in $Pvf1^{ex3}$;$Pvf2\text{-}3^{-/-}crq$>*Pvf2* triple mutants (Fig. 4G-M), but was not able to rescue lethality. *Pvf2* expression does not have to be restricted to neuroblasts: *repo-Gal4* driven *Pvf2* expression rescued brain growth and neuroblast loss in $Pvf1^{ex3}$;$Pvf2\text{-}3^{-/-}crq$>*Pvf2* mutants (Fig. 4G-M). These data show that loss of neural Pvf expression largely accounts for post-embryonic brain development defects in Pvf triple mutants.

Loss of glial Pvr causes loss of PI3K and DE-Cadherin signaling

In *Drosophila*, Pvf-Pvr signaling activates PI3K, Ras-Map kinase, Rho-Rac and Cadherin pathways (Brückner et al., 2004; Cho et al., 2002; Duchek et al., 2001; Garlena et al., 2015; McDonald et al., 2003). Genetic and cell biological approaches were used to determine which of these pathways are required for cortex glia development downstream of Pvf-Pvr. Cortex glia-specific loss of PI3K signaling, by overexpressing dp110 or dAkt RNAi or overexpressing dominant-negative mTor using cortex glia drivers, reduced larval brain size, reduced cortex glia cell numbers and induced morphogenesis defects, similar to Pvr knockdown (Fig. S10A-F). These results are consistent with published data showing that PI3K-mTor activity is required to promote cortex glia morphogenesis and support of neuroblasts (Chell and Brand, 2010; Sousa-Nunes et al., 2011; Spéder and Brand, 2018). In contrast, glial-specific knockdown of Ras-Map kinase or Rho-Rac pathway components failed to yield glial defects comparable with Pvr knockdown or induced early lethality (Fig. 1C,D; Fig. S10A,G; not shown).

Immunohistochemistry showed that glial-specific Pvr loss reduced PI3K pathway activity. To assess PI3K, I used the tGPH reporter, which is composed of GFP fused to a plextrin-homology (PH) domain that localizes to cell membranes in response to high PIP3 levels (Britton et al., 2002). *repo*>Pvr^{RNAi} and $Pvf1^{ex3}$;$Pvf2\text{-}3^{-/-}crq$>Pvr^{λ} brains showed decreased membrane-associated tGPH fluorescence in cortex glia, neuroblasts and in immature neurons compared with wild-type controls (Fig. 5A,B; Figs S13, S14A,B). To confirm this, I examined eIF4E levels, which have been used as an indicator of PI3K signaling in *Drosophila* (Hsieh and Ruggero, 2010; Song and Lu, 2011), and eIF4E was reduced in neuroblasts in *repo*>Pvr^{RNAi} and $Pvf1^{ex3}$;$Pvf2\text{-}3^{-/-}crq$>*Pvf2* mutants relative to wild type (Fig. S14C-D; not shown). Thus, Pvr loss reduced PI3K signaling cell-autonomously in glia and non-autonomously in neuroblasts and their progeny. Consistent with a requirement for PI3K signaling downstream of Pvr in glia, overexpression of constitutively active dp110 ($dp110^{CAAX}$) partially rescued effects of *repo*>Pvr^{RNAi} on brain growth and neuroblast number (Fig. 5C,D,G; Fig. S15A-C).

During larval development, glia produce ligands that stimulate PI3K signaling in neuroblasts. The insulin-like ligand *Dilp6* is expressed by subperineurial glia and cortex glia, and drives InR-PI3K signaling in neuroblasts, and *Dilp6* expression requires mTor signaling in glia (Avet-Rochex et al., 2012; Chell and Brand, 2010; Sousa-Nunes et al., 2011; Spéder and Brand, 2018). At later larval stages, cortex glia also express Jeb, a secreted ligand for the Alk RTK expressed in neuroblasts (Cheng et al., 2011). Thus, the non-autonomous effects of Pvr loss on neuroblasts may be caused by reduced Dilp6 and/or Jeb expression. Consistent with this, qPCR showed a significant reduction in *Dilp6* and *jeb* expression in larval brains from *repo*>Pvr^{RNAi}, *repo*>$Pvr^{\Delta C}$;$Pvr^{c02195/+}$ and $Pvf1^{ex3}$;$Pvf2\text{-}3^{-/-}crq$>Pvr^{λ} mutants compared with wild type (Fig. S16A,B). Dilp6 overexpression partially rescued neuroblast numbers and gross brain growth, and restored neuroblast proliferation in Pvr^{RNAi} animals (Fig. 5D,G; Fig. S16C), suggesting that activation of InR signaling, whether directly or indirectly, restores cortex glia and/or neuroblast function. In contrast, Jeb overexpression did not rescue neuroblasts or gross brain size in *repo*>Pvr^{RNAi} animals (Fig. S16C), indicating that Alk activation is insufficient to counteract Pvr loss.

PI3K signaling is required in neuroblasts to maintain growth and proliferation throughout larval development (Chell and Brand, 2010; Cheng et al., 2011; Sousa-Nunes et al., 2011), and PI3K signaling in neuroblasts is required to anchor neuroblasts in the cortex glia niche through DE-cadherin-dependent adhesion (Doyle et al., 2017). DE-Cadherin is expressed in larval central brain cortex glia and localizes at the interface of cortex glia and central brain neuroblasts, and glial DE-cadherin (DEcad) function is essential for maintenance and proliferation of neuroblasts and their progeny (Dumstrei et al., 2003; Holcroft et al., 2013). In the ovary, Pvf1-Pvr signaling regulates DE-Cadherin subcellular localization and function, perhaps directly at the membrane (McDonald et al., 2003). As Pvr is localized in cortex glial processes, perhaps Pvr-PI3K signaling regulates DE-cadherin function in cortex glia to promote anchoring, survival and/or proliferation of neuroblasts and neurons. Consistent with this, Pvr knockdown reduced DE-cadherin levels in cortex glia and non-autonomously in neuroblasts (Fig. 5C,E,F; Fig. S17), but failed to similarly reduce DE-cadherin levels in neighboring immature neurons (Fig. 5E,F). Moreover, glial-specific overexpression of DE-cadherin partially rescued cortex glia, neuroblasts and neurons in Pvr^{RNAi} animals (Fig. 5D,G-L; Fig. S15). These results indicate that cortex glia-specific Pvr loss induces an autonomous and non-autonomous reduction in DE-cadherin levels, which contributes to neuroblast loss.

Pvr signaling drives glial neoplasia

Examining the effects of Pvr gain of function, I found that Pvf2 or Pvr overexpression increased cortex glia proliferation (Fig. 6A-D; Fig. S18). Pvr^{λ} or wild-type Pvr (Pvr^{WT}) overexpression produced abnormal compact proliferative cortex glia that accumulate to enlarge the brain, which is consistent with neoplastic transformation (Fig. 6A-D). Moreover, abnormal cortex glia outcompeted neuroblasts during the 2nd to 3rd instar larval stages, such that neuroblasts were lost (Fig. 6B,E,F). To determine how loss of Pvr signaling contributed to transformation, I examined DE-cadherin expression, which was reduced in Pvr^{λ} mutant cortex glia and remaining neuroblasts in *R122*>Pvr^{λ} relative to wild type (Fig. 6E,F). Thus, in this context, neuroblasts may be lost due to reduced glial DE-cadherin function.

Development (2018) 145, dev164285. doi:10.1242/dev.164285

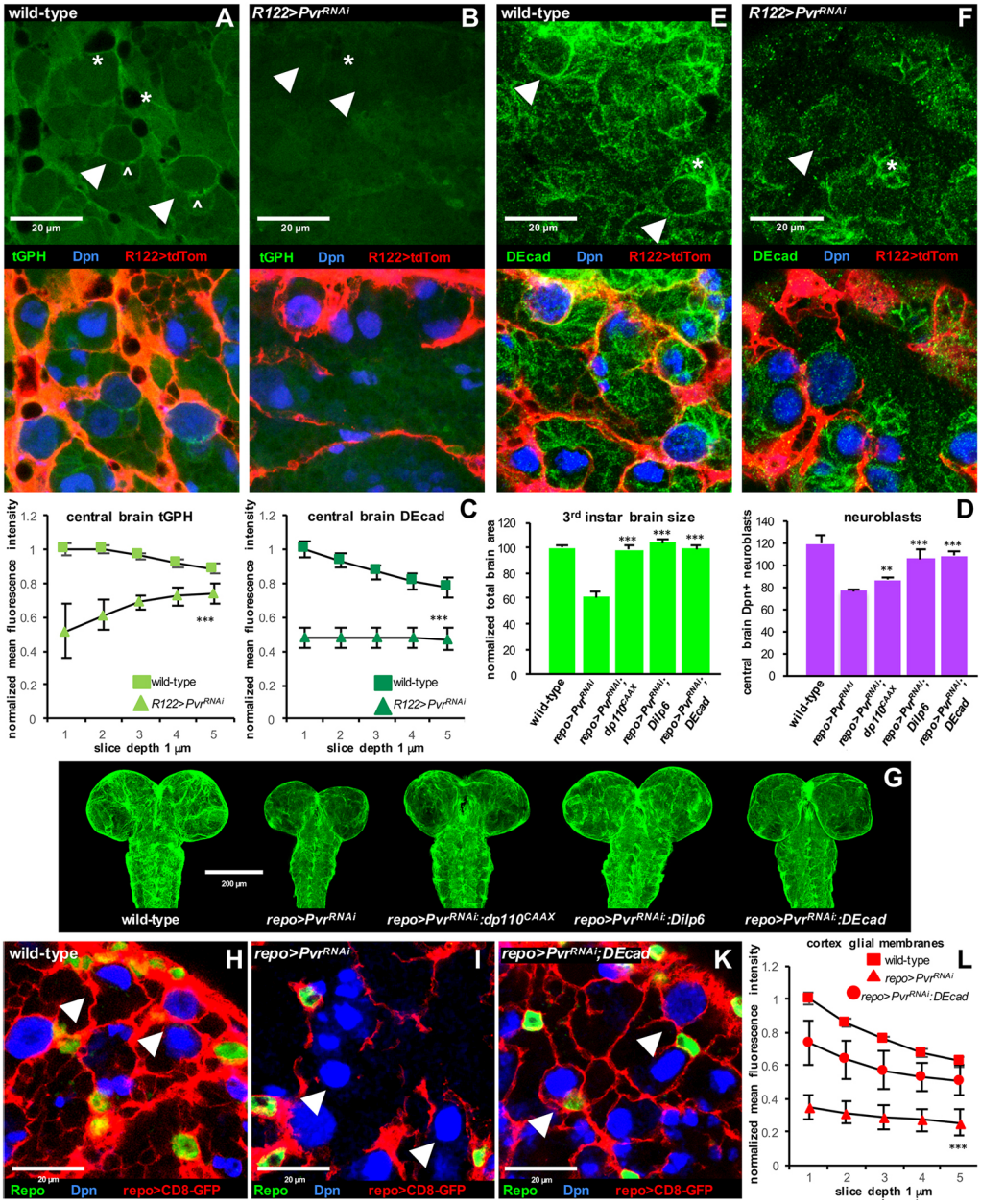

Fig. 5. Loss of glial Pvr causes cell-autonomous and non-autonomous loss of PI3K signaling. (A,B) Optical sections (2 µm) of 3rd instar brains (same scale). Green shows tGPH reporter localization; *R122>tdTom* (red) labels cortex glia membranes; Dpn (blue) labels neuroblast nuclei. (A) In wild type, membrane-associated tGPH fluorescence overlaps with glia (overlay), neuroblasts (arrowheads) and GMCs (carats). (B) *R122>Pvr^{RNAi}* brains showed reduced tGPH membrane fluorescence in glia (asterisks) and neuroblasts (arrowheads). (C) tGPH and DECad membrane fluorescence intensities and the central brain, normalized to wild-type controls, plotted over a 5 µm depth, mean intensities are significantly different between wild type (n=3) and *R122>Pvr^{RNAi}* (n=3), as determined by paired Student's t-test; ***P<0.005. Data are mean±s.e.m. (D) Brain area measured in µm^2 in optical projections of late 3rd instar brains, normalized to wild type. Wild type (n=5), *repo>Pvr^{RNAi};dp110^{CAAX}* (n=5), *repo>Pvr^{RNAi};Dilp6* (n=5) and *repo>Pvr^{RNAi};DEcad* (n=3) mutants were significantly larger than *repo>Pvr^{RNAi}* (n=6) controls, but not significantly different from each other. Neuroblasts (Dpn$^+$) in the central brain counted in 20 µm confocal z-stacks of 3rd instar brain hemispheres. *repo>Pvr^{RNAi};dp110^{CAAX}* (n=3), *repo>Pvr^{RNAi};Dilp6* (n=5) and *repo>Pvr^{RNAi};DEcad* (n=4) mutants showed a significant increase in neuroblasts relative to *repo>Pvr^{RNAi}* (n=5) controls, and were much more similar to wild type (n=5), as determined by pairwise Student's two-tailed t-tests. **P<0.05; ***P<0.005. Data are mean±s.e.m. (E,F) Optical sections (2 µm) of 3rd instar brains (same scale). Green shows DEcad-GFP reporter localization; *R122>tdTom* (red) labels cortex glia membranes; Dpn (blue) labels neuroblast nuclei. (E) In wild type, membrane-associated DEcad-GFP fluorescence overlaps with glia (overlay) and neuroblasts (arrowheads). (F) *R122>Pvr^{RNAi}* showed reduced DEcad-GFP membrane fluorescence in both glia and neuroblasts (arrowheads) compared with wild type, but retains DEcad-GFP expression in developing neurons (asterisks). Examples of full brain hemispheres shown in Fig. S17. (G) Late 3rd instar larval brains at ∼130 h AED (same scale). *repo>CD8-GFP* labels glia. *dp110^{CAAX}*, *Dilp6* and *DEcad* overexpressed by *repo-Gal4* all rescued the brain size reduction caused by glial-specific Pvr RNAi. (H-K) Optical sections (2 µm) of 3rd instar brains (same scale). *repo>tdTom* (red) labels cortex glia membranes; Repo (green) labels glial nuclei; Dpn (blue) labels neuroblast nuclei. (H) In wild type, neuroblasts are wrapped with cortex glia membranes (arrowheads), which are reduced or absent in (I) *repo>Pvr^{RNAi}* brains, causing neuroblasts to cluster together. Co-overexpression of DEcad with Pvr RNAi (K) partially rescues cortex glial cell membranes associated with neuroblasts (arrowheads). Full-brain hemispheres are shown in Fig. S15. (L) Cell membrane fluorescence intensities in cortex glia associated with neuroblasts in the central brain, normalized to wild-type control values, plotted over a 5 µm depth, mean intensities are significantly different between wild type (n=4) and *R122>Pvr^{RNAi}* (n=4), with *R122>Pvr^{RNAi};DEcad* (n=4) showing a partial rescue of glial cell membranes. Values are compared using paired Student's t-test; ***P<0.005.

Development (2018) 145, dev164285. doi:10.1242/dev.164285

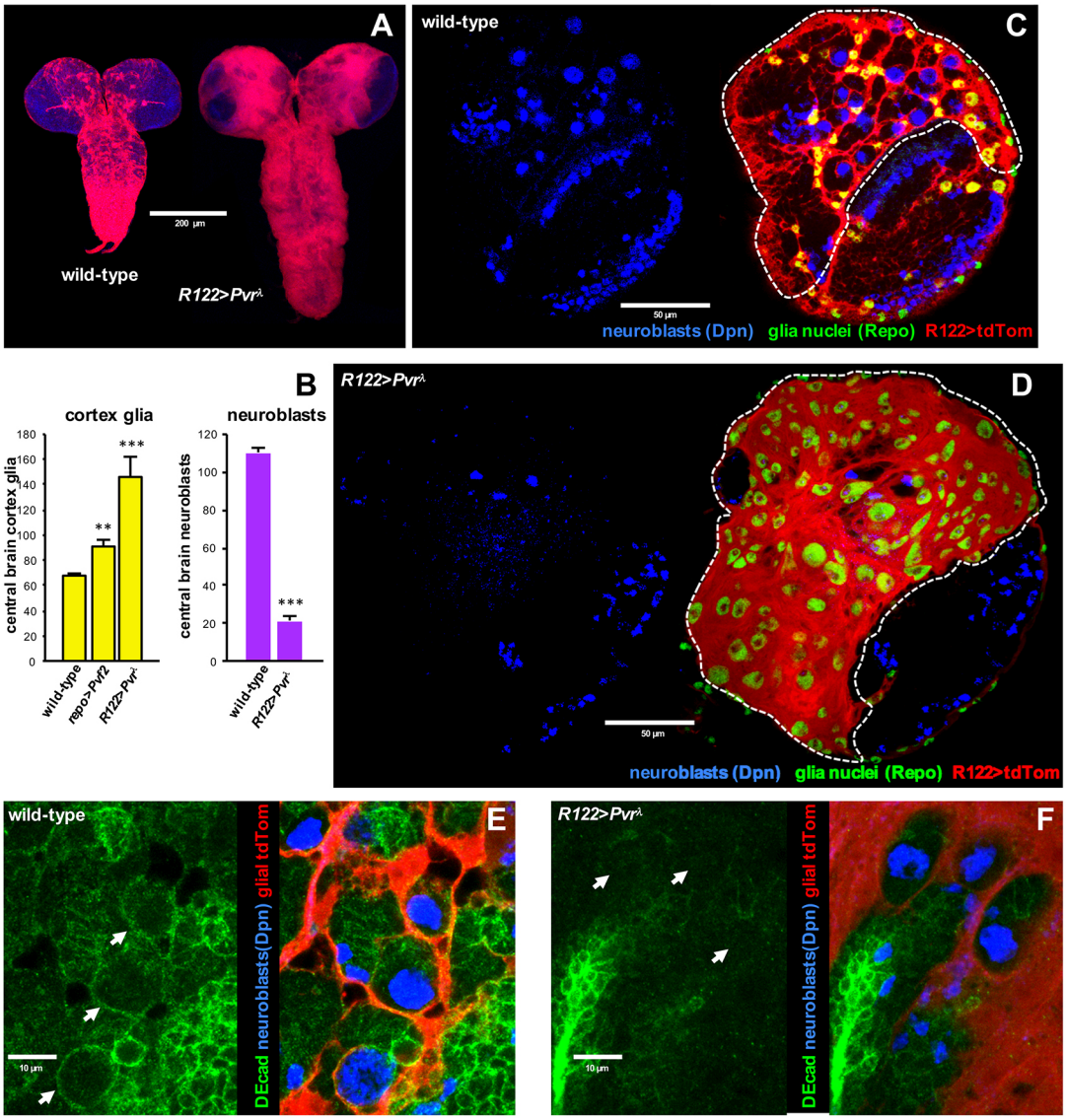

Fig. 6. Ectopic Pvf and Pvr signaling causes overproliferation of cortex glia. (A) Late 3rd instar larval brains at ∼130 h AED (same scale). *R122>tdTom* labels cortex glia (green); blue labels cell nuclei. (B) Cortex glia (R122>tdTom Repo+) in the central brain counted in 18 µm confocal *z*-stacks of late 3rd instar brain hemispheres: wild type (*n*=4), *R122>Pvf2* (*n*=6), *R122>Pvr*$^{\lambda}$ (*n*=3). Neuroblasts (Dpn^{+}) in the central brain counted in 30 µm confocal *z*-stacks of late 3rd instar brain hemispheres: wild type (*n*=5), *R122>Pvr*$^{\lambda}$(*n*=5). Values for *R122>Pvf2* and *R122>Pvr*$^{\lambda}$ brains compared with wild type; Student's two-tailed *t*-test; $^{**}P<0.05$; $^{***}P<0.005$. (C,D) Optical sections (2 µm) of 3rd instar brains (same scale). Dpn (blue) labels neuroblast nuclei; Repo (green) labels glial nuclei; *R122>tdTom* (red) labels cortex glia membranes. The central brain (dashed lines) of (D) *R122>Pvr*$^{\lambda}$ animals showed increased cortex glial cells with abnormal morphology, and decreased neuroblasts, when compared with (C) wild type. (E,F) Optical sections (2 µm) of 3rd instar brains (same scale). Green shows DEcad-GFP reporter localization; *R122>tdTom* (red) labels cortex glia membranes; Dpn (blue) labels neuroblast nuclei. (E,F) In wild type (E), neuroblasts and cortex glia show DEcad-GFP expression (arrows), see overlay (right) for glial membrane expression, which is reduced or absent in (F) *R122>Pvr*$^{\lambda}$ glia and associated neuroblasts (arrows).

In the rodent brain, PDGFR signaling regulates proliferation and differentiation of oligodendrocyte precursor cells (OPCs) (reviewed by Funa and Sasahara, 2014), which are vertebrate glial progenitor cells, and constitutive PDGFR signaling can drive malignant glial transformation in glioblastomas (GBMs) (Assanah et al., 2006; Hambardzumyan et al., 2009). GBMs, which are the most aggressive primary brain cancers in humans, are thought to arise from neuro-glial stem or progenitor cells, such as OPCs, in response to mutations that cause constitutive activation of RTKs, such as EGFR or PDGFRA (reviewed by Furnari et al., 2007). In GBMs, ectopic PDGFRA signaling cooperates with gain-of-function mutations in other RTKs, such as EGFR, to drive tumor progression (Furnari et al., 2007).

Similarly, in a *Drosophila* model of GBM in which glial progenitor cells are malignantly transformed by constitutively active *Drosophila* EGFR (dEGFR$^{\lambda}$) and dp110 (dp110^{CAAX}), Pvr knockdown suppressed glial neoplasia and eliminated SoxN-positive tumorous glia (Fig. 7A-C; Fig. S19A,B). Thus, as in human GBMs, Pvr cooperates with dEGFR. This suggests that a large proportion of tumor cells in the EGFR-PI3K *Drosophila* GBM model originate from Pvr-dependent cortex glia cells. Consistent with this interpretation, dEGFR$^{\lambda}$ and dp110^{CAAX} also drives neoplastic glial overgrowth when targeted to cortex glia: *R122>dEGFR*$^{\lambda}$*;dp110*^{CAAX} animals develop tumorous glia with neoplastic features (Fig. 7D,E).

As with Pvr-dependent transformation, abnormal cortex glia transformed by dEGFR$^{\lambda}$; dp110^{CAAX} outcompeted neuroblasts

Development (2018) 145, dev164285. doi:10.1242/dev.164285

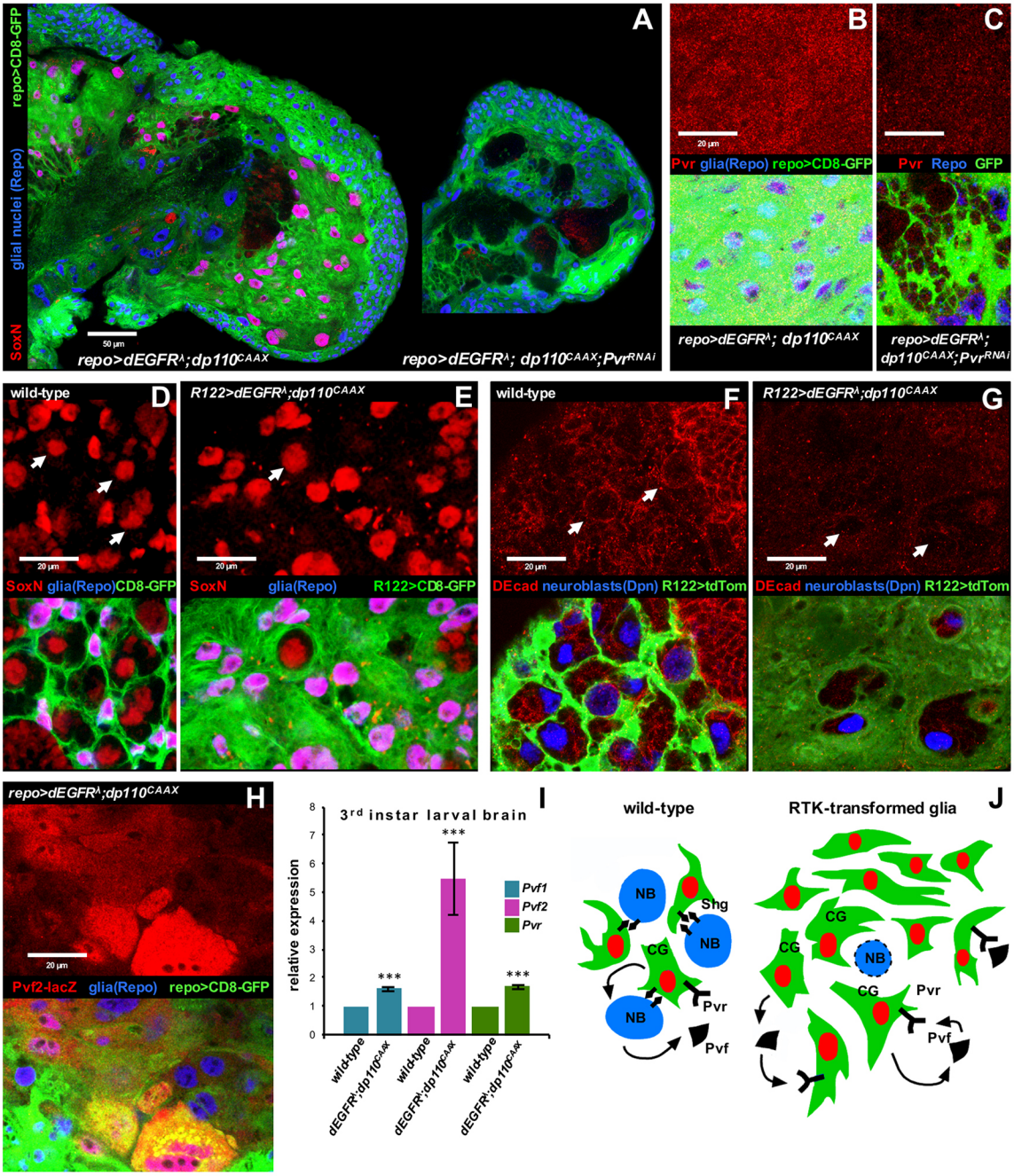

Fig. 7. Autocrine Pvr signaling drives glial neoplasia. (A) Optical sections (2 µm) mid-way through 3rd instar brain hemispheres; *repo>CD8-GFP* labels glia; Repo (blue) labels glial nuclei; SoxN labels cortex glial cell nuclei (purple) and weakly labels neuroblasts (red). Pvr knockdown reduced the number of neoplastic cortex glia, evidenced by absence of purple SoxN^{+} glial nuclei, compared with *repo>dEGFR$^{\lambda}$;dp110^{CAAX}* controls. (B,C) Optical sections (1 µm) of 3rd instar brains from (B) *repo>dEGFR$^{\lambda}$;dp110^{CAAX}* and (C) *repo>dEGFR$^{\lambda}$;dp110^{CAAX};Pvr^{RNAi}* (same scale). Repo (blue) labels glial cell nuclei; repo>CD8-GFP (green) labels glial cell bodies. Pvr protein (red) is expressed in neoplastic glial cells in *repo>dEGFR$^{\lambda}$;dp110^{CAAX}* mutants (overlay) and is dramatically reduced in *repo>dEGFR$^{\lambda}$;dp110^{CAAX};Pvr^{RNAi}* mutants. (D,E) Optical sections (2 µm) of early 3rd instar brains from (D) wild type and (E) *R122>dEGFR$^{\lambda}$;dp110^{CAAX}* (same scale). *R122>CD8-GFP* labels cortex glia; Repo labels glial nuclei (blue). SoxN^{+} neoplastic cortex glia (red in upper panels, purple in overlays) outcompete neuroblasts (weaker red; red only in overlay) in the central brain during tumorigenesis, as evidenced by loss of neuroblasts in (E) *R122>dEGFR$^{\lambda}$;dp110^{CAAX}* relative to (D) wild type. (F,G) Optical sections (2 µm) of 3rd instar brains (same scale). Green shows DEcad-GFP (false-colored red) localization; *R122>tdTom* (green) labels cortex glia membranes; Dpn (blue) labels neuroblast nuclei. In wild type (F), neuroblasts and cortex glia show DEcad expression (arrows), which is reduced or absent in (G) *R122>dEGFR$^{\lambda}$;dp110^{CAAX}* glia and associated neuroblasts (arrows). (H) Optical sections (2 µm) from *repo>dEGFR$^{\lambda}$;dp110^{CAAX}* with *Pvf2-lacZ*. *Pvf2-LacZ* (red) showed expression in neoplastic glia (red; purple-yellow in overlay) co-labeled with Repo (blue; purple in overlay) and CD8-GFP. (I) qPCR on RNA from 3rd instar brain lobes. *Pvf1*, *Pvf2* and *Pvr* expression was calculated for each genotype relative to *rp49* using the ΔΔCq method. Gene expression in *repo>dEGFR$^{\lambda}$;dp110^{CAAX}* brains normalized to wild type. Error bars show confidence intervals for gene expression, calculated using normalized ΔΔCq values for two or three replicates each. Values compared pairwise using Student's two-tailed *t*-test. ***P<0.005. (J) Model for Pvf-Pvr function. Neuroblasts (NBs, left) produce Pvfs to stimulate Pvr-PI3K-Akt signaling in cortex glia (CG). Pvr-PI3K signaling drives DE-Cadherin expression and localization in cortex glia, which promotes neuroblast maintenance and neuron survival. RTK-transformed glia (right) overexpress Pvfs, which stimulates autocrine activation of Pvr-PI3K in cortex glia, uncoupling their growth from neuroblasts. Neoplastic glia outcompete neuroblasts in the central brain.

Development (2018) 145, dev164285. doi:10.1242/dev.164285

during the 2nd to 3rd instar larval stages (Read et al., 2009), such that neuroblasts were lost (Fig. 7D,E), likely due to reduced glial DE-cadherin expression (Fig. 7F,G). Thus, Pvr-dependent neoplastic cortex glia likely no longer rely on Pvf produced by neuroblasts, which are lost. Instead, neoplastic $dEGFR^{\lambda}$;$dp110^{CAAX}$ glia express and require Pvfs: qPCR and the *Pvf2-lacZ* reporter showed that Pvf1 and Pvf2 become overexpressed in *$dEGFR^{\lambda}$; $dp110^{CAAX}$* brains, and Pvf1 RNAi partially suppressed EGFR-PI3K glial neoplasia (Fig. 7H,I; Fig. S19C). Thus, Pvf-Pvr create an autocrine loop that stimulates neoplastic transformation of cortex glia (Fig. 7J).

DISCUSSION

During post-embryonic *Drosophila* brain development, cortex glia create a microenvironment that promotes neurogenesis. I show that neuroblasts and their progeny express Pvfs, which signal through Pvr to stimulate cortex glia survival and morphogenesis, which then promotes PI3K-DE-cadherin-dependent proliferation and survival of neuroblasts and their progeny (Fig. 7K). Thus, through an RTK-PI3K-DE-Cadherin-dependent feed-forward loop, neuronal stem/progenitor cells and immature neurons actively maintain their microenvironment.

Pvf-Pvr signaling and cortex glia development and function

Previous studies of *Drosophila* neuroblast-glia interactions have focused on growth factors secreted by glia to promote neuroblast re-activation rather than on factors neuroblasts and associated progenitor cells use to shape the glial microenvironment. These studies show that the fat body, acting as an endocrine organ, produces a systemic relay signal that stimulates glial Dilp expression to drive neurogenesis in early larval stages (Britton and Edgar, 1998; Chell and Brand, 2010; Sousa-Nunes et al., 2011). My results show that neuroblasts and their progeny express Pvfs at the onset of post-embryonic neurogenesis and into late larval stages to promote Pvr-dependent niche morphogenesis and maintenance. Neuroblast Pvf expression could be initiated by Dilps or other relay signals, and understanding control of Pvf expression may reveal new mechanisms that govern post-embryonic neurogenesis.

My data show that Pvr loss-of-function impairs cortex glia morphogenesis and survival. This is consistent with previous studies showing that Pvr signaling is required for trophic support and morphogenesis in other cell types (Brückner et al., 2004; Garlena et al., 2015; Parsons and Foley, 2013). I found that loss of Pvf-Pvr function decreased PI3K signaling in cortex glia, that loss of PI3K pathway components partially phenocopies Pvf-Pvr loss of function, and that restoration of PI3K signaling in glia partially rescued the effects of Pvr knockdown. However, $dp110^{CAAX}$ overexpression did not fully rescue neuroblast loss with Pvr knockdown; this may be because receptor scaffolding is needed to facilitate localized interactions between dp110 and other signaling effectors in cortex glia, such as DE-cadherin. Alternately, other pathways downstream of Pvr may mediate interactions with effectors such as DE-cadherin. Consistent with my results, Spéder and Brand (2018) showed that reduced PI3K activity impaired cortex glia niche morphogenesis and neuroblast wrapping in the nerve cord. My results and those of Spéder and Brand seemingly conflict with those of Avet-Roche et al., which show that dp110 is not essential for cortex glia cell proliferation and/or survival. However, Avet-Roche et al. did not specifically examine the effects of reduced PI3K activity on central brain cortex glia, and instead they examined cortex glia cells throughout the brain or in the optic lobe. Differential requirements for PI3K signaling in central brain cortex glia may underlie the discrepancies between our results.

I found that cortex glia defects cause neuroblasts and immature neurons to die and/or exit the cell cycle. At later larval stages, cortex glia express Dilp6 and Jeb (Avet-Rochex et al., 2012; Cheng et al., 2011), and both Dilp6 and Jeb expression were reduced by Pvf-Pvr loss. However, Dilp6 overexpression, but not Jeb overexpression, largely rescued the cell growth and survival defects caused by Pvr knockdown. Whereas Alk is required for neuroblast proliferation, InR is required for both neuroblast proliferation and cortex glia proliferation and morphogenesis (Avet-Rochex et al., 2012; Chell and Brand, 2010; Spéder and Brand, 2018). It is possible that Dilp6 rescues Pvr loss by stimulating InR-PI3K signaling in both neuroblasts and cortex glia.

Previous studies show that extrinsic contact-dependent cues are required to polarize embryonic neuroblasts, which is essential for proper asymmetric cell division (Siegrist and Doe, 2006). DE-cadherin, a contact-dependent cue that is essential for neuroblast proliferation (Doyle et al., 2017; Dumstrei et al., 2003), showed reduced expression in cortex glia upon Pvr loss, and DE-cadherin co-overexpression largely rescued the effects of Pvr knockdown. In the *Drosophila* germline, DE-cadherin functions in homophilic adhesion between germline stem (GSCs) cells and niche cells, and this anchors GSCs to the niche to promote self-renewal and orient asymmetric cell division (Inaba et al., 2010; Song et al., 2002). Recent studies indicate that, similarly, DE-cadherin is required to mediate anchoring between neuroblasts and cortex glia (Doyle et al., 2017). Further investigation will be required to determine how DE-cadherin regulates morphogenesis and survival of cortex glia, and promotes neuroblast self-renewal. Of note, DE-cadherin levels were not as affected in immature neurons upon glial-specific Pvr loss, indicating that cortex glia may regulate neuronal survival via different mechanisms.

RTK signaling and glial tumorigenesis

My results support an evolutionarily conserved role for PDGFR signaling in *Drosophila* glial development and tumorigenesis. In the mammalian CNS, PDGFRs are essential for development of neuro-glial stem/progenitor cells (Funa and Sasahara, 2014). In human GBM, PDGFRs drive tumor initiation and migration (Fomchenko and Holland, 2007). Previous studies show that, in *Drosophila*, ectopic Pvr signaling can drive neoplastic transformation and ectopic migration of retinal glia, and these studies have led to the identification of new pathways involved in migration of human GBMs (Kim et al., 2014; Witte et al., 2009). My results show that cortex glia are also subject to neoplastic transformation, and produce tumors in response to ectopic Pvr or EGFR activity. Human GBMs, including those with EGFR mutations, co-overexpress PDGFRs and PDGFs, and these redundant RTKs, and their ligands drive GBM tumorigenesis (Fig. S20A-E, Furnari et al., 2007). My results show that RTK-driven *Drosophila* glial tumors rely on similar autocrine Pvr signaling (Fig. 7K). Thus, the glial niche can originate brain tumors, and this process involves misregulation of pathways that control niche-neural stem/progenitor cell interactions.

In the presence of neoplastic cortex glia in the central brain, neuroblasts are eliminated. Neuroblasts may be lost through cell competition, a process in which oncogene-overexpressing cells actively kill their normal neighbors in response to differences in growth factor signaling or adhesion (reviewed by

Development (2018) 145, dev164285. doi:10.1242/dev.164285

Amoyel and Bach, 2014), which in this case may be mediated by reduced DE-cadherin. In mammals, loss of normal stem/progenitor cells contributes to early stage tumorigenesis: in a mouse model of GBM, in the absence of different rates of proliferation, nascent neoplastic OPCs outcompete and eliminate normal OPCs to overtake the neurogenic niche prior to tumor emergence (Galvao et al., 2014). Although the mechanisms whereby neoplastic cells overtake the niche are unknown, elimination of normal cells may prime the microenvironment to support tumor growth (Galvao et al., 2014). Further study of interactions between normal and neoplastic neuroblasts and glia in the *Drosophila* central brain may reveal conserved mechanisms of development and tumorigenesis.

MATERIALS AND METHODS

Fly stocks, genetics and culture conditions

Drosophila stocks were obtained from the Bloomington Drosophila Stock Center unless otherwise noted as follows: $Pvf1^{ex3}$-null mutant (a gift from M. Krasnow, Stanford University, CA, USA; Cho et al., 2002); *UAS-Pvf2*, *UAS-*Pvr^{λ} and $Pvf2\text{-}3^{-/-}$ double null mutant and recombinants (gifts from E. Foley, University of Alberta, Canada; Parsons and Foley, 2013); Pvr^{c02195} mutant (a gift from D. Montell, University of California - Santa Barbara, CA, USA); *wor-Gal4* (a gift from C. Doe, University of Oregon, Eugene, OR, USA); *moody-Gal4* (a gift from R. Bainton, University of California - San Francisco, CA, USA); and *alarm-Gal4* (a gift from M. Freeman, Vollum Institute, Portland, OR, USA). NP drivers were purchased from Kyoto Stock Center. *R108-Gal4* and *R122-Gal4* cortex glial drivers were isolated in my lab in an enhancer trap screen for new glial-specific Gal4 drivers (R.D.R., unpublished). The *Pax6-EGFP* promoter fusion reporter present in MiET Minos constructs (Metaxakis et al., 2005) was isolated in my lab as a specific reporter for cortex glia in the larval brain, and, to date, all MiET insertions tested show EGFP expression in cortex glia, labeling their cell bodies and processes. Kinome-wide RNAi stocks were obtained from VDRC and all stocks tested have been previously described (Read et al., 2013).

Flies were cultured at 25°C unless otherwise noted. Complex genotypes were established by standard genetics. Larval brain phenotypes were assessed as previously described (Read et al., 2009, 2013). Briefly, for larval brain size comparisons and neurogenesis experiments, embryos were collected for all genotypes side-by-side for 12-24 h and age-matched larvae at the same stages (1st, 2nd or 3rd instars) were collected for comparison by dissection, staining and imaging with confocal fluorescence microscopy. For late 3rd instar larvae, brains were collected at 130 h (5.5 days) after egg deposition (AED).

RNAi screen

The screen was based on crosses that generated progeny containing a single RNAi construct exclusively expressed in GFP-labeled glia. Transgenes were overexpressed using the glial-specific *repo-Gal4* transcriptional driver. Screening was performed using a fluorescence stereomicroscope to visualize GFP-labeled glia in living 2nd and 3rd instar larvae, and to compare RNAi brain size phenotypes with control brain size phenotypes. Those RNAi constructs that yielded obvious brain size reductions were confirmed with confocal microscopy. However, I cannot rule out the possibility that other RNAi constructs tested have subtler glial phenotypes. In the primary screen, each positive-scoring RNAi construct was tested at least twice with *UAS-dcr* in the background (to enhance knockdown), and at least twice without *UAS-dcr* in the background to confirm reproducibility and assess penetrance. To eliminate constructs that non-specifically interfered with glial cell development, positive scoring RNAi constructs were also tested for their effects on over-all brain growth in when overexpressed in neuroblasts or neurons using *UAS-dcr;* $insc^{1407}$*-Gal4*, *UAS-dcr;* $insc^{1407}$*-Gal4; wor-Gal4*, *elav-*$Gal4^{c155}$*; UAS-dcr*, and/or *UAS-dcr; ey-Gal4*, and brains from resulting flies were scored on a fluorescence stereomicroscope and confirmed by confocal microscopy. Constructs that caused early organismal lethality were excluded from analysis. When available, dominant-negative and additional RNAi constructs were tested for candidate genes, and loss-of-function mutations were examined for brain growth phenotypes.

Immunohistochemistry and confocal imaging

Larval brains were dissected, stained and imaged as previously described (Read et al., 2009). All cell nuclei were visualized with DRAQ7 DNA dye, and actin filaments were visualized with phalloidin-Alexa-555 for low-magnification whole-brain images. Primary antibodies: rabbit anti-Pvr [1:500, a gift from D. Montell (McDonald et al., 2003)], rabbit anti-Pvr [1:500, a gift from J. Brugarolas, University of Texas Southwestern Medical Center, Dallas, TX, USA (Tran et al., 2013)], guinea pig anti-Dpn (1:500-1:1000, a gift from J. Skeath, Washington University, St Loius, MO, USA), rat anti-Dpn (1:2, a gift from C.-Y. Lee, University of Michigan, Ann Arbor, MI, USA), rabbit anti-eIF4E (1:400, a gift from P. Lasko, McGill University, Montreal, Canada), rat anti-Pvf1 [1:50-1:100, a gift from B. Shilo, Weizmann Institute of Science, Rehovot, Israel (Rosin et al., 2004)], rabbit anti-Repo (1:500, a gift from H. Reichert, University of Basel, Switzerland), mouse anti-Repo (1:10, DSHB), chicken anti-GFP (1:500, Aves), and goat or donkey anti-HRP (1:100-1:200, Jackson Immunolabs). For EdU labeling experiments, dissected brain ventral nerve cord complexes were incubated for 1 h in 10 µM EdU in Schneider's medium, fixed for 30-45 min in 4% formaldehyde 1×PBS, permeabilized in 0.3% Triton 1× PBS, followed by detection with an Alexa-647-labeled probe as per manufacturer's instructions (Click-iT EdU Imaging Kit, Life Technologies). TUNEL-labeling experiments were performed according to manufacturer's instructions. Otherwise, antibody staining was performed according to published protocols (Read et al., 2009). Fixed tissues stained for fluorescence microscopy were mounted dorsal side upwards in Vectashield (Vector Laboratories), and whole brains were imaged using confocal microscopy.

Fluorescent images were acquired with a Zeiss LSM 510 or LSM 700. Confocal projections were prepared using Zen. Images were subject to standard processing using Zen or Photoshop (Read et al., 2009). Nuclear Dpn stains (guinea pig antibody) were corrected for particulate background fluorescence in Zen using the median filter. For experiments in which protein levels and/or localization were compared between genotypes (tGPH, eIF4E and DEcadGFP), brain samples were isolated from age-matched animals grown side by side, and brains were prepared and imaged in parallel using the same microscope and confocal imaging settings, and processed using Zen and Photoshop in the same manner. All experimental and control brains shown in each figure panel grouping are from age-matched representative animals grown alongside each other, unless noted otherwise. For figures with low-magnification whole larval brain images, brains were imaged separately and panels were assembled in Photoshop or PowerPoint. Image quantification procedures are described in the supplementary Materials and Methods.

RNA sequencing and human tumor genomics

Primary glioblastoma (GBM) neurosphere cultures were isolated from surgical specimens donated for research with informed consent from patients, and were collected and used according to recognized ethical guidelines in a protocol (IRB00045732) approved by the Institutional Review Board at Emory University. GBM cultures were maintained as per published protocols (Read et al., 2013). RNAseq was performed for each culture as per commercial procedures (Beckman Coulter), and primary sequencing data were subject to bioinformatic processing (Winship Bioinformatics Core), assembly, and gene and transcript expression analysis using TopHat and Cufflinks. mRNA expression data for primary glioblastoma tumor tissue specimens and for lower grade glioma tumor tissue specimens (grade II and III gliomas) were obtained from TCGA datasets through the cBio Portal (www.cbioportal.org, PanCancer Atlas dataset). Additional details are provided in the supplementary Materials and Methods.

qPCR

Drosophila brains were dissected away from the body, ventral nerve cord and all other larval tissues. RNA was prepared from Trizol as per

manufacturer's instructions (Life Technologies), cDNAs were prepared as per manufacturer's instructions (Bio-Rad), and qPCR was run on a BioRad CFX96 Touch as per manufacturer's instructions. Primer sequences for *Drosophila* loci were obtained from DSRC FlyPrimerBank (www.flyrnai.org/flyprimerbank). For each comparison, each experiment included technical replicates (in duplicate) and, when possible, two separate primers were used for each gene to confirm expression data (bar graphs show only results for one primer). Results from *gapdh* and *rp49* were used as controls to normalize relative gene expression levels as per standard ΔΔCq methods as described by the manufacturer's instructions.

Statistics

Experimental data were compared pairwise using Student's two-tailed *t*-test or, for the membrane intensity datasets, paired Student's *t*-test. Graphs show averages for each value presented. Error bars show s.e.m. unless otherwise noted.

Acknowledgements

I thank Coston Rowe for technical assistance, Jeffrey Olson for GBM tissues, and Brendan Parsons and Edan Foley for Pvr and Pvf mutants.

Competing interests

The author declares no competing or financial interests.

Author contributions

Conceptualization: R.D.R.; Methodology: R.D.R.; Validation: R.D.R.; Formal analysis: R.D.R.; Investigation: R.D.R.; Resources: R.D.R.; Data curation: R.D.R.; Writing - original draft: R.D.R.; Writing - review & editing: R.D.R.; Project administration: R.D.R.; Funding acquisition: R.D.R.

Funding

This research was funded by the National Institute of Neurological Disorders and Stroke (R00 NS065974). Deposited in PMC for release after 12 months.

Data availability

The RNA-sequencing data have been deposited in Gene Expression Omnibus under Accession Number GSE122679.

Supplementary information

Supplementary information available online at
http://dev.biologists.org/lookup/doi/10.1242/dev.164285.supplemental

References

Amoyel, M. and Bach, E. A. (2014). Cell competition: how to eliminate your neighbours. *Development* **141**, 988-1000.

Assanah, M., Lochhead, R., Ogden, A., Bruce, J., Goldman, J. and Canoll, P. (2006). Glial progenitors in adult white matter are driven to form malignant gliomas by platelet-derived growth factor-expressing retroviruses. *J. Neurosci.* **26**, 6781-6790.

Avet-Rochex, A., Kaul, A. K., Gatt, A. P., McNeill, H. and Bateman, J. M. (2012). Concerted control of gliogenesis by InR/TOR and FGF signalling in the Drosophila post-embryonic brain. *Development* **139**, 2763-2772.

Awasaki, T., Lai, S.-L., Ito, K. and Lee, T. (2008). Organization and postembryonic development of glial cells in the adult central brain of Drosophila. *J. Neurosci.* **28**, 13742-13753.

Bainton, R. J., Tsai, L. T.-Y., Schwabe, T., DeSalvo, M., Gaul, U. and Heberlein, U. (2005). moody encodes two GPCRs that regulate cocaine behaviors and blood-brain barrier permeability in Drosophila. *Cell* **123**, 145-156.

Bjornsson, C. S., Apostolopoulou, M., Tian, Y. and Temple, S. (2015). It takes a village: constructing the neurogenic niche. *Dev. Cell* **32**, 435-446.

Britton, J. S. and Edgar, B. A. (1998). Environmental control of the cell cycle in Drosophila: nutrition activates mitotic and endoreplicative cells by distinct mechanisms. *Development* **125**, 2149-2158.

Britton, J. S., Lockwood, W. K., Li, L., Cohen, S. M. and Edgar, B. A. (2002). Drosophila's insulin/PI3-kinase pathway coordinates cellular metabolism with nutritional conditions. *Dev. Cell* **2**, 239-249.

Brückner, K., Kockel, L., Duchek, P., Luque, C. M., Rørth, P. and Perrimon, N. (2004). The PDGF/VEGF receptor controls blood cell survival in Drosophila. *Dev. Cell* **7**, 73-84.

Chell, J. M. and Brand, A. H. (2010). Nutrition-responsive glia control exit of neural stem cells from quiescence. *Cell* **143**, 1161-1173.

Cheng, L. Y., Bailey, A. P., Leevers, S. J., Ragan, T. J., Driscoll, P. C. and Gould, A. P. (2011). Anaplastic lymphoma kinase spares organ growth during nutrient restriction in Drosophila. *Cell* **146**, 435-447.

Cho, N. K., Keyes, L., Johnson, E., Heller, J., Ryner, L., Karim, F. and Krasnow, M. A. (2002). Developmental control of blood cell migration by the Drosophila VEGF pathway. *Cell* **108**, 865-876.

Choi, N.-H., Kim, J.-G., Yang, D.-J., Kim, Y.-S. and Yoo, M.-A. (2008). Age-related changes in Drosophila midgut are associated with PVF2, a PDGF/VEGF-like growth factor. *Aging Cell* **7**, 318-334.

Coutinho-Budd, J. C., Sheehan, A. E. and Freeman, M. R. (2017). The secreted neurotrophin Spatzle 3 promotes glial morphogenesis and supports neuronal survival and function. *Genes Dev.* **31**, 2023-2038.

Doe, C. Q. (2008). Neural stem cells: balancing self-renewal with differentiation. *Development* **135**, 1575-1587.

Doherty, J., Logan, M. A., Tasdemir, O. E. and Freeman, M. R. (2009). Ensheathing glia function as phagocytes in the adult Drosophila brain. *J. Neurosci.* **29**, 4768-4781.

Doyle, S. E., Pahl, M. C., Siller, K. H., Ardiff, L. and Siegrist, S. E. (2017). Neuroblast niche position is controlled by Phosphoinositide 3-kinase-dependent DE-Cadherin adhesion. *Development* **144**, 820-829.

Duchek, P., Somogyi, K., Jékely, G., Beccari, S. and Rørth, P. (2001). Guidance of cell migration by the Drosophila PDGF/VEGF receptor. *Cell* **107**, 17-26.

Dumstrei, K., Wang, F. and Hartenstein, V. (2003). Role of DE-cadherin in neuroblast proliferation, neural morphogenesis, and axon tract formation in Drosophila larval brain development. *J. Neurosci.* **23**, 3325-3335.

Fomchenko, E. I. and Holland, E. C. (2007). Platelet-derived growth factor-mediated gliomagenesis and brain tumor recruitment. *Neurosurg. Clin. N Am.* **18**, 39-58.

Funa, K. and Sasahara, M. (2014). The roles of PDGF in development and during neurogenesis in the normal and diseased nervous system. *J. Neuroimmune Pharmacol.* **9**, 168-181.

Furnari, F. B., Fenton, T., Bachoo, R. M., Mukasa, A., Stommel, J. M., Stegh, A., Hahn, W. C., Ligon, K. L., Louis, D. N., Brennan, C. et al. (2007). Malignant astrocytic glioma: genetics, biology, and paths to treatment. *Genes Dev.* **21**, 2683-2710.

Galvao, R. P., Kasina, A., McNeill, R. S., Harbin, J. E., Foreman, O., Verhaak, R. G. W., Nishiyama, A., Miller, C. R. and Zong, H. (2014). Transformation of quiescent adult oligodendrocyte precursor cells into malignant glioma through a multistep reactivation process. *Proc. Natl. Acad. Sci. USA* **111**, E4214-E4223.

Garlena, R. A., Lennox, A. L., Baker, L. R., Parsons, T. E., Weinberg, S. M. and Stronach, B. E. (2015). The receptor tyrosine kinase Pvr promotes tissue closure by coordinating corpse removal and epidermal zippering. *Development* **142**, 3403-3415.

Hambardzumyan, D., Amankulor, N. M., Helmy, K. Y., Becher, O. J. and Holland, E. C. (2009). Modeling adult gliomas using RCAS/t-va technology. *Transl. Oncol.* **2**, 89-95.

Heino, T. I., Kärpänen, T., Wahlström, G., Pulkkinen, M., Eriksson, U., Alitalo, K. and Roos, C. (2001). The Drosophila VEGF receptor homolog is expressed in hemocytes. *Mech. Dev.* **109**, 69-77.

Holcroft, C. E., Jackson, W. D., Lin, W.-H., Bassiri, K., Baines, R. A. and Phelan, P. (2013). Innexins Ogre and Inx2 are required in glial cells for normal postembryonic development of the Drosophila central nervous system. *J. Cell Sci.* **126**, 3823-3834.

Homem, C. C. F. and Knoblich, J. A. (2012). Drosophila neuroblasts: a model for stem cell biology. *Development* **139**, 4297-4310.

Hsieh, A. C. and Ruggero, D. (2010). Targeting eukaryotic translation initiation factor 4E (eIF4E) in cancer. *Clin. Cancer Res.* **16**, 4914-4920.

Inaba, M., Yuan, H., Salzmann, V., Fuller, M. T. and Yamashita, Y. M. (2010). E-cadherin is required for centrosome and spindle orientation in Drosophila male germline stem cells. *PLoS ONE* **5**, e12473.

Kim, S. N., Jeibmann, A., Halama, K., Witte, H. T., Walte, M., Matzat, T., Schillers, H., Faber, C., Senner, V., Paulus, W. et al. (2014). ECM stiffness regulates glial migration in Drosophila and mammalian glioma models. *Development* **141**, 3233-3242.

Li, H.-H., Kroll, J. R., Lennox, S. M., Ogundeyi, O., Jeter, J., Depasquale, G. and Truman, J. W. (2014). A GAL4 driver resource for developmental and behavioral studies on the larval CNS of Drosophila. *Cell Rep.* **8**, 897-908.

McDonald, J. A., Pinheiro, E. M. and Montell, D. J. (2003). PVF1, a PDGF/VEGF homolog, is sufficient to guide border cells and interacts genetically with Taiman. *Development* **130**, 3469-3478.

McKimmie, C., Woerfel, G. and Russell, S. (2005). Conserved genomic organisation of Group B Sox genes in insects. *BMC Genet.* **6**, 26.

Metaxakis, A., Oehler, S., Klinakis, A. and Savakis, C. (2005). Minos as a genetic and genomic tool in Drosophila melanogaster. *Genetics* **171**, 571-581.

Parsons, B. and Foley, E. (2013). The Drosophila platelet-derived growth factor and vascular endothelial growth factor-receptor related (Pvr) protein ligands Pvf2 and Pvf3 control hemocyte viability and invasive migration. *J. Biol. Chem.* **288**, 20173-20183.

Pereanu, W., Shy, D. and Hartenstein, V. (2005). Morphogenesis and proliferation of the larval brain glia in Drosophila. *Dev. Biol.* **283**, 191-203.

Read, R. D., Cavenee, W. K., Furnari, F. B. and Thomas, J. B. (2009). A drosophila model for EGFR-Ras and PI3K-dependent human glioma. *PLoS Genet.* **5**, e1000374.

Read, R. D., Fenton, T. R., Gomez, G. G., Wykosky, J., Vandenberg, S. R., Babic, I., Iwanami, A., Yang, H., Cavenee, W. K., Mischel, P. S. et al. (2013). A kinome-wide

RNAi screen in Drosophila Glia reveals that the RIO kinases mediate cell proliferation and survival through TORC2-Akt signaling in glioblastoma. *PLoS Genet.* **9**, e1003253.
Rosin, D., Schejter, E., Volk, T. and Shilo, B. Z. (2004). Apical accumulation of the Drosophila PDGF/VEGF receptor ligands provides a mechanism for triggering localized actin polymerization. *Development* **131**, 1939-1948.
Siegrist, S. E. and Doe, C. Q. (2006). Extrinsic cues orient the cell division axis in Drosophila embryonic neuroblasts. *Development* **133**, 529-536.
Song, Y. and Lu, B. (2011). Regulation of cell growth by Notch signaling and its differential requirement in normal vs. tumor-forming stem cells in Drosophila. *Genes Dev.* **25**, 2644-2658.
Song, X., Zhu, C. H., Doan, C. and Xie, T. (2002). Germline stem cells anchored by adherens junctions in the Drosophila ovary niches. *Science* **296**, 1855-1857.
Sousa-Nunes, R., Yee, L. L. and Gould, A. P. (2011). Fat cells reactivate quiescent neuroblasts via TOR and glial insulin relays in Drosophila. *Nature* **471**, 508-512.
Spéder, P. and Brand, A. H. (2014). Gap junction proteins in the blood-brain barrier control nutrient-dependent reactivation of Drosophila neural stem cells. *Dev. Cell* **30**, 309-321.
Spéder, P. and Brand, A. H. (2018). Systemic and local cues drive neural stem cell niche remodelling during neurogenesis in Drosophila. *eLife* **7**, e30413.
Tran, T. A., Kinch, L., Pena-Llopis, S., Kockel, L., Grishin, N., Jiang, H. and Brugarolas, J. (2013). Platelet-derived growth factor/vascular endothelial growth factor receptor inactivation by sunitinib results in Tsc1/Tsc2-dependent inhibition of TORC1. *Mol. Cell. Biol.* **33**, 3762-3779.
Witte, H. T., Jeibmann, A., Klämbt, C. and Paulus, W. (2009). Modeling glioma growth and invasion in Drosophila melanogaster. *Neoplasia* **11**, 882-888.